

0.34 V_T AlGa_N/Ga_N-on-Si Large Schottky Barrier Diode With Recessed Dual Anode Metal

Hyun-Soo Lee, Dong Yun Jung, Youngrak Park, Jeho Na, Hyun-Gyu Jang, Hyoung-Seok Lee, Chi-Hoon Jun, Junbo Park, Sang-Ouk Ryu, Sang Choon Ko, and Eun Soo Nam

Abstract—A large Ga_N-Schottky barrier diode (SBD) with a recessed dual anode metal is proposed to achieve improved the forward characteristics without a degradation of the reverse performances. Using optimized dry etch condition for a large device, the electrical characteristics of the device are demonstrated when applying the recessed dual anode metal and changing the recess depths. The device size and channel width are 4 mm² and 63 mm, respectively. The 16-nm recessed dual anode metal SBD has a turn-ON voltage of 0.34 V, a breakdown voltage of 802 V, and a reverse leakage current of 1.82 μA/mm at -15 V. The packaged SBD exhibits a forward current of 6.2 A at 2 V and a reverse recovery charge of 11.54 nC.

Index Terms—AlGa_N/Ga_N on Si, Schottky barrier diode (SBD), recess dual anode metal, low turn-on voltage.

I. INTRODUCTION

GALLIUM nitride (Ga_N) power devices are drawing greater attention in high-power switching applications owing to their superior power density, efficiency, and switching speed [1]. To achieve high efficiency and a small size in a power-conversion system, a low turn-on voltage (V_T), low on-resistance (R_{on}) and low reverse recovery of the diode are very important [2]. Various technologies to improve the performance of an SBD have recently been studied. Researches to reduce on-resistance and to reduce surface leakage current, such as SiO₂, SiN_x, Al₂O₃ dielectric film, have been investigated [3]. In addition, studies on recess etching in the anode region and recess depth control have been actively conducted owing to the capability of recessed SBDs to reduce the V_T without an increase in the leakage current [4]–[6]. However, for large device fabrication, the dry etch conditions including a uniform etch profile, a reproducible etch rate, and a small amount of plasma damage are very difficult and

challenging to control. In addition, the damage occurring during the etching process may seriously degrade the device performance. Meanwhile, an anode composed of two metals with different work functions was reported to achieve a better trade-off between the forward and reverse characteristics. Although dual metal can be used as an anode to reduce V_T, the reverse leakage current is increased at the same time. Thus, it is very difficult to control an SBD whose anode is made solely of dual metal [7], [8]. Therefore, dual anode metal along with recess etch in anode region have been demonstrated to effectively control both the forward and reverse characteristics [9].

In this letter, we propose a dry etch condition that results in a uniform etch profile, an accurate etch rate, and very little plasma damage. Moreover, using this dry etch condition, we demonstrate the use of large 63-mm SBDs with a recessed dual anode metal structure, which have an ultralow turn-on voltage, and superior forward and reverse characteristics. Also, this letter includes the measured electrical characteristics of recessed dual anode metal SBDs with different recess depth and the packaged SBD to analyze the electrical characteristics in the high power regime.

II. DEVICE FABRICATION

The epitaxial layers of a AlGa_N/Ga_N SBD were grown on a 4-in Si (111) wafer, where the wafer median sheet resistance was 527 Ω/□. The wafer consists of a 3-to-4-μm Ga_N buffer layer, a 20-nm Al_{0.25}G_{0.75}N barrier, and a 1.25-nm undoped Ga_N layer. A mesa isolation with an etching depth of 300 nm was applied through inductively coupled plasma reactive ion etching (ICP RIE) using a BCl₃/Cl₂ gas mixture. To form an ohmic contact in cathode and anode, a Ti/Al/Ni/Au ohmic metal was deposited using e-beam evaporation on the cathode and anode concurrently, followed by rapid thermal annealing at 900 °C for 50 s in N₂ ambient. The transfer contact and specific contact resistivity were 1.08 Ω · mm and 2.4 × 10⁻⁵ Ω · cm², respectively. To observe different electrical characteristics of the proposed SBDs with varying recess depths, a recess process using the same ICP RIE and etch conditions was carried out. The etching profile is usually not uniform in larger devices because the same structure cannot be scaled up to larger dimensions. Problems such as epitaxial defects, non-uniformity, and uneven etching conditions have plagued larger devices. Moreover, an uneven etch surface morphology can result in an increase in the surface leakage current. Therefore, to obtain dry etch with a uniform etch profile, accurate etch rate, little plasma damage, and with an even surface morphology for larger devices, we optimized the conditions by changing the ICP power, RF power, gas feed

Manuscript received August 12, 2015; revised August 25, 2015; accepted August 27, 2015. Date of publication August 31, 2015; date of current version October 21, 2015. This work was supported in part by the Institute for Information and Communications Technology Promotion within the Ministry of Science, ICT and Future Planning through the Korean Government under Grant B0101-15-0132, in part by the Next Generation Optical and Electrical Module Technology for Smart Data Center under Grant B0132-15-1006, and in part by the Development of High Efficiency Ga_N-Based Key Components and Modules for Base and Mobile Stations. The review of this letter was arranged by Editor T. Egawa. (Corresponding author: Sang Choon Ko.)

H.-S. Lee is with the Electronics and Telecommunications Research Institute, Daejeon 34129, Korea, and also with the Department of Electronics and Electrical Engineering, Dankook University, Yongin 16890, Korea.

D. Y. Jung, Y. Park, J. Na, H.-G. Jang, H.-S. Lee, C.-H. Jun, J. Park, S. C. Ko, and E. S. Nam are with the Electronics and Telecommunications Research Institute, Daejeon 34129, Korea (e-mail: scko@etri.re.kr).

S.-O. Ryu is with the Department of Electronics and Electrical Engineering, Dankook University, Yongin 16890, Korea.

Color versions of one or more of the figures in this letter are available online at <http://ieeexplore.ieee.org>.

Digital Object Identifier 10.1109/LED.2015.2475178

TABLE I
ICP-RIE PROCESS CONDITION

Sample	ICP power	RF power	Gas (BCl ₃ /Cl ₂)	Pressure	Etch rate
(a)	300 W	5 W	3/18 sccm	5 mTorr	~17 Å/s
(b)	300 W	3 W	3/18 sccm	5 mTorr	~1.2 Å/s
(c)	200 W	3 W	16/3 sccm	5 mTorr	~1.0 Å/s
(d)	50 W	3 W	16/3 sccm	5 mTorr	~0.6 Å/s
(e)	50 W	3 W	16/3 sccm	10 mTorr	~0.3 Å/s

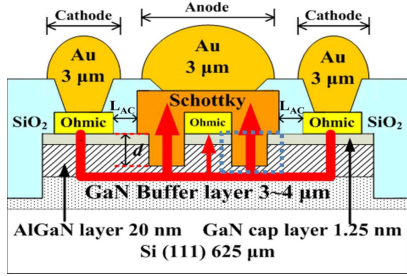


Fig. 1. Cross-section of the proposed AlGaN/GaN on Si SBD with recessed dual anode metal.

rate, and the chamber pressure. The dry etch conditions used for ICP RIE are summarized in Table I.

Under the lowest etch rate condition of (e) in Table I, the minimum RMS roughness of the etched surface was measured as 0.29 nm. The recess depths d measured through AFM were 16, 20, 24 nm, as shown in Fig. 1. Next, a Ni/Au Schottky metal for the anode was deposited, and a SiO₂ passivation layer of 700 nm was then deposited using PECVD. The distance between the anode and cathode, L_{AC} , is 15 μm. The width of ohmic metal and Schottky metal are both 15 μm. After removing the SiO₂ passivation layer in the anode and cathode regions using wet etching with a buffered oxide etchant, a 3-μm-thick Ti/Au metal was finally plated as the contact metal. Fig. 1 shows the structure of the proposed SBD and the flow of electrons.

In structures with recessed anode, the 2-D electron gas (2DEG) density under the anode electrode depends strongly on the recess depth. And the threshold voltage increases is expected by increasing the recess depth due to the reduction of 2DEG density. The leakage current is effectively controlled by the selectively reduced 2DEG density under the Schottky metal of the anode region. To effectively control the leakage current and obtain the positive threshold voltage, more than half of the AlGaN layer of the anode region should be etched [10]. In other words, the leakage current is significantly increased when the recess depth is less than 12 nm. To achieve a better trade-off between the forward and reverse characteristics, we selected recess depth to be more than 16 nm. When a small forward bias is applied to the anode, electrons flow from the cathode to the ohmic metal in the anode. In addition, when a forward bias that can turn on the Schottky contact under the recessed anode region is applied to the anode, electrons run through the Schottky metal. Additional electrons through the ohmic-to-ohmic path result in a high forward current and a very low V_T . In addition, when a reverse bias is applied to the anode, the 2DEG channel is effectively depleted by the Schottky metal under the recessed

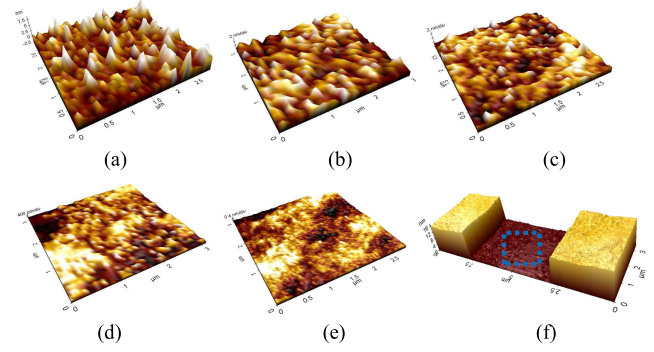


Fig. 2. (a)-(e) AFM images from the different ICP RIE process condition shown in Table I (the roughness of (a) 1.7 nm, (b) 1 nm, (c) 0.68 nm, (d) 0.38 nm, (e) 0.29 nm) and (f) a whole structure image of the recessed dual anode metal.

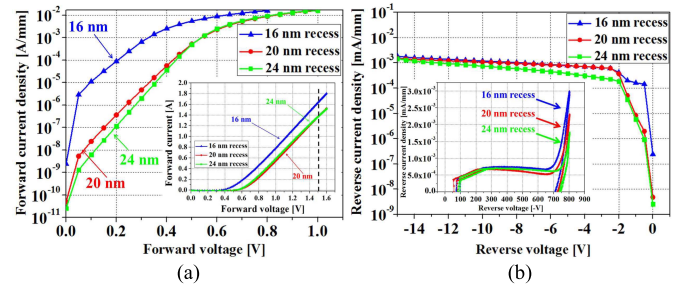


Fig. 3. (a) Forward (inset: high current measurement) and (b) reverse (inset: breakdown voltage measurement) I-V curves by varying the recess depths.

anode region. Consequently, forward characteristics are greatly improved without an increase in the leakage current [9].

III. RESULTS AND DISCUSSION

Fig. 2 shows AFM images of the RMS roughness of the etched surface when changing the ICP RIE process conditions. As shown in Fig. 2(e), the optimized dry etch conditions with a uniform etch profile and very little plasma damage can decrease the surface leakage current. In addition, an etch rate of ~0.3 Å/s allows the recess depth to be accurately controlled.

Fig. 3 shows the current-voltage (I-V) characteristics of the proposed large recessed dual anode metal SBDs with various recess depths. The I-V characteristics were measured using an HP4155 and a Tektronix 370A for low and high currents, respectively. The measured electrical characteristics are summarized in Table II.

An SBD with a 16-nm recess depth exhibits the lowest V_T of 0.34 V and the highest forward current of 1.63 A at 1.5 V as shown in Fig. 3(a). The electrical characteristics of the 20-nm and 24-nm (fully) recessed SBDs are very similar. This phenomenon can be explained by the fact that, for a device whose recessed depths under the anode region are more than 20 nm, electrons tend to go through the Schottky metal, instead of through the ohmic metal in the anode. This is the reason why electrons that flow to ohmic metal in anode are suppressed by Schottky metal under recessed anode region. Fig. 3(b) shows the reverse I-V curve and breakdown voltage (BV) of the proposed 16-nm recessed SBD. In comparison with the 20- and 24-nm recessed SBDs, its leakage current is almost the same. In other words, although the forward performance of the 16-nm recessed SBD is superior to that of the other recessed SBDs, the degradation of the reverse characteristics is negligible. We can see that 16-nm recessed dual anode

TABLE II
DEVICE CHARACTERISTICS

Recess depth	V_T (V)	I_F (A) at 1.5 V	I_R (μ A/mm) at -15 V	BV (V)
16 nm	0.34	1.63	1.82	802
20 nm	0.55	1.36	1.5	800
24 nm	0.54	1.37	1.45	803

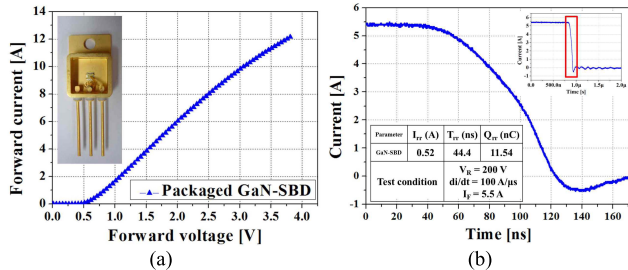


Fig. 4. Measured (a) forward I-V and (b) reverse-recovery waveforms of the TO-packaged GaN-SBD with 16-nm recessed dual anode metal.

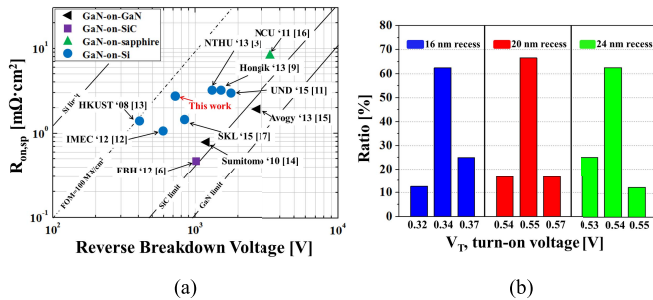


Fig. 5. (a) The benchmark plot of BV versus $R_{ON,SP}$ of GaN power diode on GaN/SiC/sapphire/Si substrate. The extracted $R_{ON,SP}$ of the fabricated device in this letter is $5 \text{ m}\Omega \cdot \text{cm}^2$ and (b) the histogram of the turn-on voltage by varying the recess depths.

metal SBD has the lower V_T than other recessed SBDs by the ohmic-to-ohmic junction effect as shown from 0 V to 0.2 V in Fig. 3(a) and from -2 V to 0 V in Fig. 3(b). In addition, the BV did not change when changing the recess depth.

Fig. 4(a) shows the measured forward I-V characteristics and a photograph of the packaged 16-nm recessed GaN-SBD, which exhibits a high forward current of 6.2 A at 2 V. A typical reverse recovery wave form of the proposed SBD is shown in Fig. 4(b). The switching conditions are shown in the table in Fig. 4(b). The measured recovery current (I_{rr}), time (T_{rr}), and charge (Q_{rr}) are 0.52 A, 44.4 ns, and 11.54 nC, respectively.

Fig. 5(a) shows the benchmark of $R_{ON,SP}$ (Specific On-resistance) vs. BV of the state-of-art GaN diode on different substrate. Fig. 5(b) exhibits the histogram of the V_T , which is significantly influenced by recess depth, to show the uniformity about the recess process in this letter.

IV. CONCLUSION

We studied dry etch conditions for a uniform etch profile, accurate etch rate, and very little plasma damage in the anode region. Using optimized conditions, we fabricated a recessed dual anode metal GaN-SBD with a channel width of 63 μm . The large fabricated SBD with a 16-nm recessed etch depth exhibited superior forward and reverse electrical characteristics, and was shown to be suitable for high efficiency and small form factor power conversion systems.

REFERENCES

- [1] B. J. Baliga, "Trends in power semiconductor devices," *IEEE Trans. Electron Devices*, vol. 43, no. 10, pp. 1717–1731, Oct. 1996. DOI: 10.1109/16.536818
- [2] B. Hughes, Y. Y. Yoon, D. M. Zehnder, and K. S. Boutros, "A 95% efficient normally-off GaN-on-Si HEMT hybrid-IC boost-converter with 425-W output power at 1 MHz," in *Proc. IEEE CSICS*, Oct. 2011, pp. 1–3. DOI: 10.1109/CSICS.2011.6062460
- [3] Y.-W. Lian, Y.-S. Lin, J.-M. Yang, C.-H. Cheng, and S. S. H. Hsu, "AlGaIn/GaN Schottky barrier diodes on silicon substrates with selective Si diffusion for low onset voltage and high reverse blocking," *IEEE Electron Device Lett.*, vol. 34, no. 8, pp. 981–983, Aug. 2013. DOI: 10.1109/LED.2013.2269475
- [4] Y. Yao, J. Zhong, Y. Zheng, F. Yang, Y. Ni, Z. He, Z. Shen, G. Zhou, S. Wang, J. Zhang, J. Li, D. Zhou, Z. Wu, B. Zhang, and Y. Liu, "Current transport mechanism of AlGaIn/GaN Schottky barrier diode with fully recessed Schottky anode," *Jpn. J. Appl. Phys.*, vol. 54, pp. 011001-1–011001-6, Jan. 2015. DOI: 10.7567/JJAP.54.011001
- [5] Y. Park, J.-J. Kim, W. Chang, H.-G. Jang, J. Na, H. Lee, H.-Y. Cha, J. K. Mun, S. C. Ko, and E. S. Nam, "Low onset voltage of GaN on Si Schottky barrier diode using various recess depths," *Electron. Lett.*, vol. 50, no. 16, pp. 1165–1167, Jul. 2014. DOI: 10.1049/el.2014.1747
- [6] E. Bahat-Treidel, O. Hilt, R. Zhytnytska, A. Wentzel, C. Meliani, J. Würfl, and G. Tränkle, "Fast-switching GaN-based lateral power Schottky barrier diodes with low onset voltage and strong reverse blocking," *IEEE Electron Device Lett.*, vol. 33, no. 3, pp. 357–359, Mar. 2012. DOI: 10.1109/LED.2011.2179281
- [7] T.-F. Chang, C.-F. Huang, T.-Y. Yang, C.-W. Chiu, T.-Y. Huang, K.-Y. Lee, and F. Zhao, "Low turn-on voltage dual metal AlGaIn/GaN Schottky barrier diode," *Solid-State Electron.*, vol. 105, pp. 12–15, Mar. 2015. DOI: 10.1016/j.sse.2014.11.024
- [8] S. Yoshida, J. Li, N. Ikeda, and K. Hataya, "AlGaIn/GaN field effect Schottky barrier diode (FESBD)," *Phys. Status Solidi (C)*, vol. 2, no. 7, pp. 2602–2606, May 2005. DOI: 10.1002/pssc.200461300
- [9] J.-G. Lee, B.-R. Park, C.-H. Cho, K.-S. Seo, and H.-Y. Cha, "Low turn-on voltage AlGaIn/GaN-on-Si rectifier with gated ohmic anode," *IEEE Electron Device Lett.*, vol. 34, no. 2, pp. 214–216, Feb. 2013. DOI: 10.1109/LED.2012.2235403
- [10] W. Saito, Y. Takada, M. Kuraguchi, K. Tsuda, and I. Omura, "Recessed-gate structure approach toward normally off high-voltage AlGaIn/GaN HEMT for power electronics applications," *IEEE Trans. Electron Devices*, vol. 53, no. 2, pp. 356–362, Feb. 2006. DOI: 10.1109/TED.2005.862708
- [11] M. Zhu, B. Song, M. Qi, Z. Hu, K. Nomoto, X. Yan, Y. Cao, W. Johnson, E. Kohn, D. Jena, and H. G. Xing, "1.9-kV AlGaIn/GaN lateral Schottky barrier diodes on silicon," *IEEE Electron Device Lett.*, vol. 36, no. 4, pp. 375–377, Apr. 2015. DOI: 10.1109/LED.2015.2404309
- [12] S. Lenci, B. D. Jaeger, L. Carbonell, J. Hu, G. Mannaert, D. Wellekens, S. You, B. Bakeroot, and S. Decoutere, "Au-free AlGaIn/GaN power diode on 8-in Si substrate with gated edge termination," *IEEE Electron Device Lett.*, vol. 34, no. 8, pp. 1035–1037, Aug. 2013. DOI: 10.1109/LED.2013.2267933
- [13] W. Chen, K.-Y. Wong, W. Huang, and K. J. Chen, "High-performance AlGaIn/GaN lateral field-effect rectifiers compatible with high electron mobility transistors," *Appl. Phys. Lett.*, vol. 92, no. 25, pp. 253501-1–253501-3, Jun. 2008. DOI: 10.1063/1.2951615
- [14] Y. Saitoh, K. Sumiyoshi, M. Okada, T. Horii, T. Miyazaki, H. Shiomi, M. Ueno, K. Katayama, M. Kiyama, and T. Nakamura, "Extremely low on-resistance and high breakdown voltage observed in vertical GaN Schottky barrier diodes with high-mobility drift layers on low-dislocation-density GaN substrates," *Appl. Phys. Exp.*, vol. 3, no. 8, pp. 081001-1–081001-3, Aug. 2010. DOI: 10.1143/APEX.3.081001
- [15] I. C. Kizilyalli, A. P. Edwards, H. Nie, D. Disney, and D. Bour, "High voltage vertical GaN p-n diodes with avalanche capability," *IEEE Trans. Electron Devices*, vol. 60, no. 10, pp. 3067–3070, Oct. 2013. DOI: 10.1109/TED.2013.2266664
- [16] G.-Y. Lee, H.-H. Liu, and J.-I. Chyi, "High-performance AlGaIn/GaN Schottky diodes with an AlGaIn/AlN buffer layer," *IEEE Electron Device Lett.*, vol. 32, no. 11, pp. 1519–1521, Nov. 2011. DOI: 10.1109/LED.2011.2164610
- [17] Q. Zhou, Y. Jin, J. Mou, X. Bao, Y. Shi, Z. Liu, J. Li, W. Chen, C. Sun, and B. Zhang, "Over 1.1 kV breakdown low turn-on voltage GaN-on-Si power diode with MIS-Gated hybrid anode," in *Proc. IEEE 27th Int. Symp. Power Semicond. Devices IC's (ISPSD)*, May 2015, pp. 369–372. DOI: 10.1109/ISPSD.2015.7123466